BOREAL ENVIRONMENT RESEARCH 20: 335–349
ISSN 1239-6095 (print) ISSN 1797-2469 (online)

Helsinki 26 June 2015

Increased needlefall and defoliation in Norway spruce induced by warm and dry weather

Svein Solberg[1)]*, Dan Aamlid[1)], Ole E. Tveito[2)] and Sofus Lystad[2)]

[1)] *Norwegian Forest and Landscape Institute, Høgskoleveien 12, N-1432 Ås, Norway (*corresponding author's e-mail: sos@skogoglandskap.no)*
[2)] *Norwegian Meteorological Institute, P.O. Box 43, Blindern, N-0313 Oslo, Norway*

Received 26 Sep. 2014, final version received 2 Feb. 2015, accepted 3 Feb. 2015

Solberg S., Aamlid D., Tveito O.E. & Lystad S. 2015: Increased needlefall and defoliation in Norway spruce induced by warm and dry weather. *Boreal Env. Res.* 20: 335–349.

Analyses of a time-series of needlefall data showed enhanced needlefall due to unusually warm and dry weather in southeastern Norway during 1986–2000. Needlefall was sampled routinely in ten stands of older *Picea abies* as part of long-term forest monitoring. Mixed linear models were developed for brown and green needlefall separately. Both the brown and the green needlefall had clear seasonal variations, peaking in October and May, respectively. In addition, the needlefall was correlated with weather conditions. Unusually dry summers were followed by increased brown needlefall in the autumns and winters, and unusually high temperatures were accompanied by increased amounts of green needlefall, in particular in the winter. Using the models, we found that unusually warm and dry weather during these 15 years likely caused an overall surplus of needlefall. Even though the brown needlefall was the dominant fraction of the needlefall, the surplus of green needlefall was of larger magnitude. The results suggest that unusually warm winters and dry summers were the main cause of increased crown defoliation during these years.

Introduction

In the 1980s and 1990s there was a widespread belief that air pollution was causing a forest decline in Europe, while now it appears that this was not the case and climatic factors, in particular drought, have been more important. Severe air pollution effects were seen in some heavily polluted areas such as the Ore mountains having annual mean SO_2 concentrations in air above 90 μg m^{-3} (Wentzel, 1982, Liebhold and Drechsler, 1991). An extensive forest monitoring program was established in Europe in the mid-1980s as a response to the concern for air pollution effects (Lorenz 1995). However, the presence of a widespread forest decline caused by air pollution was severely questioned at that time (Kandler and Innes 1995). This is backed up by a recent review (De Vries *et al*. 2014), which concluded that relationships between air pollution and crown condition were weak and limited in time and space, while climatic factors appeared to be more important drivers. From a philosophical viewpoint Roll-Hansen (2002) concluded that the belief in forest death from acid rain was an unnecessary misunderstanding, where science was unfortunately replaced by a consensus based belief.

During the first 15 years of forest monitoring in Norway defoliation of Norway spruce (*Picea abies*) increased in the southeastern part of the country. The effect of long-range air pollutants

Editor in charge of this article: Jukka Pumpanen

was one candidate explanation because this was the region receiving the highest deposition of anthropogenic sulphur and nitrogen compounds. However, no relationship was found between air pollution and crown condition (Solberg and Tørset 1997), and based on relationships with climatic data Solberg (2004) concluded that summer drought appeared to be the main cause. Drought is known to generate a number of damage types and effects in spruce, including needle loss (Gruber 1990, Christiansen 1992), dying of buds and branches (Aronsson *et al*. 1978), deficiency of K, Mg and other nutrients (Wehrmann 1961, Dambrine *et al*. 1993), reduced growth (Spiecker 1986), root mortality, and attacks by *Armillaria* spp. (Whitney and Timmer 1983) and bark beetles (Worrell 1983). In a recent project on top dieback, which is another damage type observed in southeast Norway, summer drought was again found to be the primary cause. Scattered, well-growing individuals, having a sudden decline from top downwards, appeared to be particularly vulnerable to cavitation from drought stress by having large, thin-walled tracheids and weak control on stomata closure as seen from ^{13}C and ^{18}O isotope analyses (Hentschel *et al*. 2014, Rosner *et al*. 2014).

The hypothesis of this study is the one proposed by Solberg (2004), i.e. that the increasing defoliation seen during 1988–2001 in southeast Norway was caused by summer droughts, which incited increased needlefall in the autumns. Excellent data were available for this, i.e. needlefall data routinely collected during these years at the so-called intensively monitored plots, as well as weather data from the Norwegian meteorological office. The hypothesis is partly backed up by several existing studies of needlefall in Norway spruce, which have shown seasonal variation and increased needlefall after unusual weather conditions, like summer drought or high winter temperatures (Mork 1942, Rehfuess and Rodenkirchen 1984, Heiniger and Schmid 1989, Gruber 1990, Livsey and Barklund 1993). However, the presently available needlefall data provided the possibility for more detailed analyses, where brown and green needlefall are separated.

The objective of this study was to investigate the amount of needlefall in Norway spruce in southeast Norway, and to clarify the influence of climatic factors. More specifically, to (1) quantify needlefall and its seasonal variation, (2) identify climatic factors influencing it, and (3) investigate whether warmth and drought could explain the increased defoliation observed during the 1980s and 1990s.

Material and methods

Study area and field plots

This study was based on needlefall data gathered from intensively monitored forest plots in southeastern Norway between 58°N and 61°N (Table 1). The plots were part of the Monitoring Programme for Forest Damage in Norway which was established in 1985 (Horntvedt *et al*. 1992), and of the pan-European network of intensive monitoring plots (ICP Forests Level II plots, Lorenz *et al*. 1997). Here, we selected plots in old, Norway spruce stands. About 90% of the trees in the plots were Norway spruce. The plot size was 0.1 ha. During the monitoring period no forest management was carried out in the plot or in a buffer zone around them.

Plot data

Litterfall has been routinely collected since 1986. Two sampling periods and sampling methods have been used:

1. In the summer and snow-free period, the samples were gathered monthly into 10 ventilated bags randomly located within the plot. The bags were mounted on a circular, steel frame with a radius of 22.5 cm and hanged 1 m above the forest floor.
2. In the winter, all collected material constituted one sample. Collection periods varied in length among plots and years depending on the duration of the snow cover. A square sampler (0.5 m × 0.5 m, wall height 10 cm) was placed directly on the ground.

The beginning and the end dates were recorded for each sample; from this we obtained needlefall flux given in kg ha^{-1} day^{-1} (Table 2).

Table 1. Plot characteristics.

Plot	Altitude (m a.s.l.)	Long. °E	Lat. °N	Age (year)[1)]	Stem number per ha	Stem volume (m^3 ha^{-1})	Volume growth (m^3 ha^{-1} $year^{-1}$)	Site index[2)]
Birkenes	198	8.24	58.38	105	1127	350	6.9	14.0
Fagernes	480	9.22	61.00	91	1897	313	8.5	14.3
Fyresdal	460	8.15	59.31	136	1674	219	3.5	9.5
Hurdal	275	11.08	60.37	63	707	344	14.2	17.7
Langtjern	560	9.74	60.37	168	1756	335	6.9	7.2
Lardal	170	9.87	59.45	117	952	355	4.5	14.4
Nordmoen	204	11.11	60.25	85	567	312	7.9	18.4
Prestebakke	150	11.53	58.98	87	840	536	13.2	21.5
Søgne	30	7.86	58.10	58	1364	528	13.9	20.5
Valle	280	7.57	59.05	119	1346	274	4.2	11.9

[1)] At breast height for the year 1990. [2)] According to the Norwegian system H40, which denotes top height at an age of 40 years at breast height.

The samples brought in the laboratory were immediately dried at 105 °C for 48 hours, and sorted manually into a fine litter sub-sample (mostly needles, but also flowers, seeds, bark fragments etc.) and a coarse litter sub-sample (mostly branches and twigs). The fine litter was then manually spread out in an even and thin layer on a plate, and the mass of sub-fractions such as brown spruce needles, green spruce needles and spruce flowers was visually assessed by specially trained staff. From this we obtained data on the mass of brown and green needle fall. The assessments were regularly controlled on randomly selected samples by manual sorting into the sub-fractions followed by weighing.

Throughout the study we kept and analysed the brown and green needlefall data separately, because differences in phenology and causal factors were expected for these fractions.

Crown defoliation was assessed for all trees in the plots annually during 1986–2000. This was done in the autumn by two observers according to international guidelines (Anon. 1989). It represents the percentage of foliage missing in comparison with the expected amount for a healthy tree at the site. Defoliation was averaged for each plot and each year, based on non-suppressed Norway spruce trees, i.e. Kraft classes 1–3.

Weather data

The Norwegian Meteorological Institute estimated meteorological data for each forest plot, by geographic interpolation of the weather station data. Temperature and precipitation were obtained as monthly residuals from 1961–1990 mean values, and expressed as deviations from the mean (temperature) and percentages of the mean (precipitation). Interpolating the residuals is a robust approach, since the variables are normalised and therefore are suited for spatial interpolation. The data in the Norwegian Meteorological Institute's climate archive were used to establish monthly maps of temperature and precipitation residuals from the 1961–1990 monthly normal values. The residual was defined at each observation station, and these values were used in a spatial interpolation to derive a continuous residual map covering all Norway with a spatial

Table 2. Sampling period and mean needlefall (kg ha^{-1} day^{-1}).

Plot	Sampling period	Needlefall	
		brown	green
Birkenes	June 1986–Dec. 2000	2.87	0.60
Fagernes	June 1987–Oct. 2000	2.98	0.59
Fyresdal	June 1987–Oct. 1994	2.00	0.57
Hurdal	Mar. 1997–Oct. 2000	3.11	0.37
Langtjern	June 1986–Oct. 2000	1.91	0.24
Lardal	June 1988–Nov. 2000	2.68	0.60
Nordmoen	June 1986–Oct. 2000	3.08	0.46
Prestebakke	June 1986–Oct. 2000	4.02	1.41
Søgne	Aug. 1987–Nov. 2000	4.12	1.92
Valle	Aug. 1988–Sep. 1999	2.12	0.37

resolution of 1 km × 1 km. The spatial interpolation method used was TOPOGRID (ESRI 2001), which for this purpose showed good performance. From this gridded representation, values for each of the forest plots were estimated for each month.

Combining the climate residual values with the 1961–1990 normal values gave absolute values at the monitoring plots. The 1961–1990 temperature normals used were the Nordic Temperature Maps (Tveito *et al*. 2000), while the precipitation normals were based on gridded representations of the precipitation maps in the National Atlas of Norway (Førland 1993).

For the period and the plots under study, precipitation was generally slightly higher than normal in the winter and slightly lower in May (Table 3). For all months, considerable variation occurred with values from near zero to thre–four times the 1961–1990 normal value. The temperatures were generally above the 1961–1990 normal, in particular in winter. For January and February, temperature deviations up to almost 10° above normal occurred (Table 3).

In addition to temperature and precipitation, we also used Palmer drought severity index, PDSI, as a measure of climatic drought (Palmer 1965). This index is based on meteorological data as well as estimated evapotranspiration and a soil water balance model including water runoff, water loss and water recharge. The water balance model is based on the standing timber volume, vegetation type, soil type, altitude and slope. First, a normal, or mean, water balance for the period 1961–1990 was estimated for each 12-month period. The Palmer indices were then calculated as deviations of these monthly normal values for the investigated period. A Palmer PDSI value greater than 4 expresses extreme wetness, zero indicates normal wetness or drought, while less than –4 identifies extreme drought. It should be emphasized that the Palmer values are standardised to each plot and only reflect deviations from the normal at this actual plot.

Table 3. Monthly meteorological means (minimum–maximum) for the period 1986–2000 for the 10 monitoring plots. Precipitation is given as percentage of, and temperature as deviation (Δt) from the 1961–1990 average.

Month	Precipitation	Δt
January	115 (12–284)	2.1 (–7.7–9.6)
February	127 (1–451)	2.3 (–5.7–9.5)
March	114 (4–266)	1.3 (–4.5–5.7)
April	120 (3–340)	0.7 (–2.2–2.8)
May	74 (0–188)	0.4 (–2.6–3.3)
June	113 (3–296)	–0.4 (–4.1–3.7)
July	94 (7–372)	0.5 (–2.5–4.7)
August	112 (6–245)	0.3 (–2.4–5.3)
September	90 (6–220)	0.2 (–2.8–4.2)
October	99 (19–280)	–0.1 (–3.8–3.5)
November	103 (19–473)	0.7 (–3.3–6.2)
December	108 (10–257)	1.0 (–4.7–5.1)

Analyses

The length of the winter sampling varied between plots and years. Prior to the statistical analyses we standardized the sampling periods by defining 8 standard sampling periods, containing monthly samples from May to November and one winter sample for December–April. Most of the litterfall samples fitted to these standard periods; however, some did not. Those were assigned to the standard periods by splitting or combining their data as follows: Any monthly samples within the standard winter period were combined with the other winter sample data. In cases where the winter samples started before December or lasted past April, we assigned the mean needlefall flux as monthly samples outside the standard winter period.

The needlefall samples were assigned to standard dates, being either on day 15 of the actual month or on 15 February for winter samples. The needlefall fluxes were recalculated into percentages of the long-term mean needlefall flux for each plot.

In order to identify relationships between weather conditions and needlefall, we first carried out a screening based on correlation analyses. We did this for various alternatives, i.e. with both monthly and seasonal values and including lagged effects. We used Spearman's rank-order correlation which is suitable and robust against outlier data. Based on these initial trial analyses, we retained the most promising relationships, based on aggregated seasonal weather data for

winter, summer and autumn. Spring weather data and spring needlefall data were excluded due to none or minor relationships. We retained relationships if the weather and needlefall data were from the same season or if the needlefall data lagged after the weather data. The winter weather data were combined with needlefall from the same winter, as well as the following summer and autumn. The summer weather data were combined with needlefall data from the same summer, as well as the following autumn and winter. The autumn weather data were combined with needlefall from the same autumn, as well as the following winter and summer.

Based on this screening of relationships, we derived the strongest weather variable for explaining brown needlefall and the strongest weather variable for explaining green needlefall. The relationships were then fitted to more sophisticated models. The idea with these models is that they should be close to the data generating biological mechanisms, and that correlations in time and space between the observations should be handled appropriately, enabling hypotheses testing. An appropriate tool for this was weighted, mixed, linear models using the MIXED procedure in SAS (Littell *et al.* 1996). In comparison with ordinary least squares (OLS), they have the advantage that dependencies between the observations can be included in the model by selecting an appropriate variance and covariance structure. We expected two types of dependencies between the observations, i.e. events occurring at the regional scale and a temporal autocorrelation (*see* below for further details). The parameter estimation was carried out with a maximum likelihood iterative procedure. Hypothesis testing on the variables was obtained with likelihood-ratio tests (Schabenberger and Pierce 2002), i.e. the change in log-likelihood along with a step-wise inclusion of variables. This means that a given variable was included in the model if this generated a sufficiently large change in log-likelihood:

$$-2\ln(\Delta\text{Likelihood}) > \chi^2_{n,0.05}, \qquad (1)$$

where n is the change in the number of parameters. We used an analysis of covariance model structure, meaning that each sampling period (month or winter) had its own intercept and its own regression slope. The observations were reasonably close to a Gaussian distribution. However, in these models we ln-transformed the needlefall data because of heteroscedasticity, i.e. the residual error variance increased with increasing needlefall. This transformation stabilized the variance over the range of needlefall values. The brown needlefall, Y_{ijk}, was fitted to the model

$$\ln(Y_{ijk}) = \beta_0 + \beta_{1i} + \beta_{2i} p_j + u_{ij} + e_{ijk} \qquad (2)$$

where β_0 denotes an overall intercept, β_{1i} denotes the intercept of the sampling period (month) i, and β_{2i} denotes the regression coefficient of needlefall against summer drought in that sampling period. Here i indexes the eight sampling periods ($i = 1, \ldots, 8$) for a one year long sequence starting with the July to November monthly samplings (i = 1–5), followed by the entire winter period December–April (i = 6), and the following May and June monthly samples (i = 7 and 8). The k indexes the plots ($i = 1, \ldots, 10$). Since the number of days varied among the samples, all observations were weighted with the number of days in that sampling period. The variable p_j was the selected weather variable, being the sum of precipitation during summer (May–August) in percent of the 1961–1990 normal value. Here j indexes the July–June sampling years ($j = 1, \ldots, 15$), where the sampling year 1986/1987 takes the value j = 1, and so on until 2000/2001 with j = 15.

The variance–covariance model included u_{ij} and e_{ijk}, which were assumed to be Gaussian zero-mean variables. The random effect u_{ij}, which can be called "timepoint", represents disturbances common for all the plots. This could be any regional event, such as a storm or a fungal disease affecting needlefall over the entire region. In the present data set, there were 119 timepoints: June 1986, July 1986, August 1986, and so until the winter of 2001. This random effect had the variance σ_t^2. In the error term e_{ijk}, we modelled an autocorrelation in time within each plot. We here applied the "spatial power law" variance–covariance structure (Littell *et al.* 1996), which models the correlation between two observations to decrease with increasing

time difference. This autocorrelation results from the fact that the effect of drought, or any other factor, upon needlefall is likely to be spread over some time. The covariance between two observations at times t_1 and t_2, is modelled as $\sigma^2\rho^{|t_1 - t_2|}$, where ρ is an autoregressive parameter assumed to satisfy $|\rho| < 1$ and σ^2 is an overall variance.

Green needlefall was handled similarly. It was fitted to a fairly similar model as brown needlefall

$$\ln(Y_{ijk}) = \beta_0 + \beta_{1i} + \beta_{2i}t_{ij} + u_{ij} + e_{ijk} \quad (3)$$

with the difference that here the selected weather variable was t_{ij}, which was the temperature deviation from the 1961–1990 normal in the same period (month) as litterfall was collected. This means that we here searched for an instant response to unusually warm weather.

Estimates from ln-transformed models are known to have a bias when converted back to the non-logarithmic form. Hence, for the presentation of the results, the model predictions were transformed back to a non-logarithmic form. We corrected the predicted needlefall values using a fixed factor, λ as follows:

$$\lambda = \Sigma(\text{observed} \times \text{days})/\Sigma(\text{predicted} \times \text{days}) \quad (4)$$

After this correction, the predicted weighted mean equalled the observed weighted mean.

If dry and warm weather prevailed in the period under study and led to increased needlefall, this was likely to have caused defoliation of tree crowns. If this was a major cause of defoliation, then the surplus of needlefall caused by dry or warm weather should correspond to the changes in defoliation. For every point in time when sampling occurred, we used Eqs. 2 and 3 to predict brown and green needlefall with the actual values of the meteorological variables averaged across plots. We then replaced the actual values with the 1961–1990 normal values and obtained estimates of what the needlefall would have been in normal weather. For this, we obtained estimates of the surplus needlefall caused by unusually dry and warm weather. These surplus needlefall values were aggregated over time, and this gave estimates of the accumulated surplus needlefall during the period 1986–2000 caused by unusually dry and warm weather.

For visualization of the data we used "least squares means" (LSMEANS, Anon. 1990: 891–1686) rather than raw data. This was necessary because the litterfall sampling periods varied somewhat between plots, and because some plots were established after 1986 and some were terminated before 2000. The LSMEANS are the best available estimates of what the data would have been had all plots been investigated for the entire study period and the litterfall sampling had had identical sampling periods each year. LSMEANS were obtained from two-way analyses of variance models:

$$Y_{ij} = \beta_{1i} + \beta_{2j} + e_{ij} \quad (5)$$

where Y_{ij} is a needlefall or defoliation variable, β_{1i} represents the mean value of plot i, β_{2j} represents the mean value at time point j (i.e. a sampling period of litterfall or a year of defoliation), and e_{ij} represents the residual error.

Results

General findings

The needlefall flux varied among plots, with mean values ranging from 2.2 to 6.0 kg ha^{-1} day^{-1} (Table 2). The lowest value was at the site Langtjern, which in this study was a low-productivity site at the highest altitude, having low productivity and low stand density. The highest value was found for Søgne, located in a high-productivity and dense stand in the lowlands of southernmost Norway. The mean needlefall flux calculated across the plots was 3.6 kg ha^{-1} day^{-1}. On average, brown and green needlefall constituted 84% and 16%, respectively, of the total needlefall in the plots. These fractions were fairly stable from plot to plot, with brown needlefall varying from 68% to 89%. The needlefall varied over the years, and two periods of high needlefall were recorded: one in 1991–1993 and the other in 1997–2000 (Fig. 1). Two other characteristics in the time series were apparent: the brown needlefall peaked in autumn, and the relatively high fraction of green

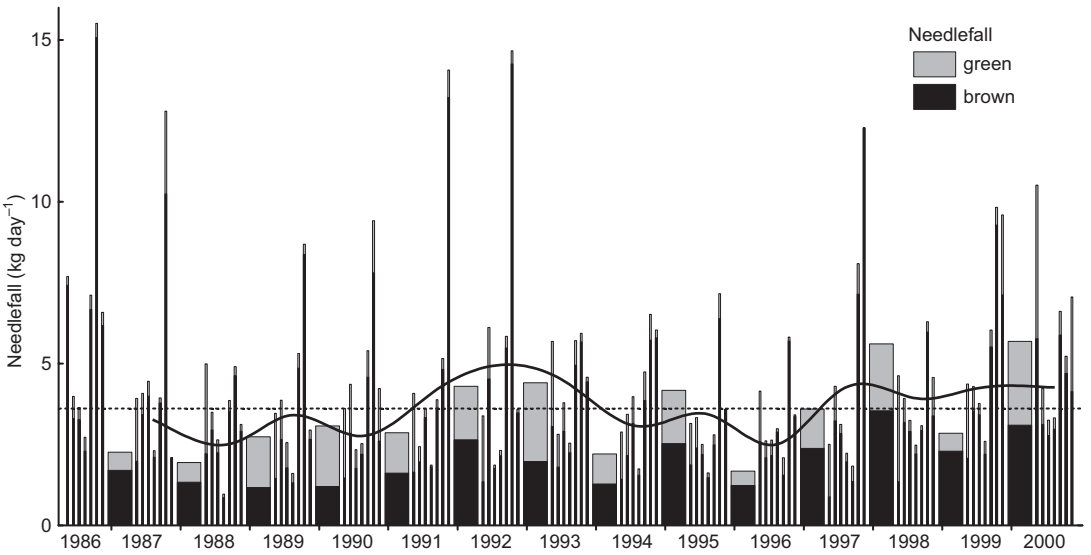

Fig. 1. The needlefall time-series-based least squares means. The bar widths correspond to the lengths of the sampling periods. The mean flux of 3.6 kg ha^{-1} day^{-1} is shown with a dotted line, and the annual totals are shown with a solid line.

needles was recorded in winter. The analyses of variance models behind these LSMEANS data were good, in the sense that the two effects in the model were able to explain a high fraction of the variance, i.e. having $r^2 = 0.70$ and $r^2 = 0.52$, respectively, for brown and green needlefall.

The peak events, consisting mainly of brown needles, occurred frequently in the autumns. This was evident in 1986–1989, 1991–1992, 1997 and 1999. The highest peak was recorded in October 1986, with 15 kg ha^{-1} day^{-1} of almost entirely brown needles. Two other peaks were recorded in November 1991 and October 1992, also being comprised of almost entirely brown needles, with 13 and 14 kg ha^{-1} day^{-1} needlefall, respectively. The latter of these events was observed in most of the plots, with a maximum value at Søgne (49 kg ha^{-1} day^{-1}). A peak was then seen in all plots with values from 11 to 49 kg ha^{-1} day^{-1}, except at Langtjern, which is a more high elevation plot, having 1 kg only. Autumnal peaks were observed in all years, and varied between the months of September, October and November. However, magnitudes of the peaks varied a lot, and the total autumn needlefall was low in some years, i.e. 1988, 1996 and 1998.

The high needlefall period in 1991–1993 was mostly due to excessive shedding of brown needles in the two peaks in the autumns of 1991 and 1992, as well as in the winter in between. However, also, a high amount of green needles from the next winter, 1992–1993, contributed significantly to the overall high needlefall in this period. The second, markedly high needlefall period, 1997–2000, was also mostly due to unusually high shedding of brown needles, i.e. the peaks in the autumns of 1997 and 1999, as well as in the winters of 1997–1998 and 1999–2000. Also, considerable amounts of green needles from the latter winter contributed clearly. Thus, of prime importance for understanding the high needlefall, and its possible relationships to observed crown defoliation, is to understand the dynamics and the drivers for the brown needlefall.

Brown needlefall and weather conditions

Brown needlefall made up the majority of the total needlefall, i.e. 84% (Table 2). The correlation analyses indicated that brown needlefall appeared to increase after warm and dry summers (Table 4). A reduced needlefall was recorded in such summers, however; this was by far outweighed by being followed by a considerable increase in the autumnal peak, and partly

also a winter increase. This apparent warmth and drought effect was most clearly seen in the models based on the Palmer drought severity index. However, the models based on rainfall and temperature deviations from the 30-years' normal also supported this finding. The climate variable most strongly correlated with the dominating autumnal needlefall was summer (May–August) precipitation expressed as percentage of the 30 years' normal, (Spearman's $r = 0.40$). A crude overview of the patterns of relationships in the data set is given in Table 4.

The more sophisticated model in Eq. 2 supported the correlation analyses, and provided more details. All the variables used in the model were all statistically significant at the 1% level (Table 5). The brown needlefall had a seasonal pattern with high values in the autumn, and peaking in October (Fig. 2). After dry summers this seasonal pattern was more pronounced, with increases in the following autumn and in the winter. On the other hand, moist summers were followed by reduced brown needlefall in the autumn and winter. After a summer that received only 50% of normal precipitation, the model predicted brown needlefall to be 22% higher as compared with that after a normal summer, when summed up from July to the June of the following year. This means that the brown needlefall peak following a dry summer is not the normal

Table 4. Overview of the relationships between climate variables and needlefall, based on Spearman's rank order correlations between needlefall in a given season expressed as percentage of the long-term average needlefall, and a series of climate variables for the same season and two preceding seasons (lagged effects). ↑ = warm or dry condition is related to increased needlefall, and ↓ = warm or dry condition is related to reduced needlefall; the symbols are presented only if the correlation coefficient was > 0.2 or < –0.2. For each combination of climate and needlefall, three alternative climate variables are used: lowest monthly value, mean monthly value and maximum monthly value. Rain% is the precipitation expressed as percentage of the 30-year mean value, Δtemp is the temperature deviation from the 30-year mean value, Palmer is the value of the palmer drought severity index (PDSI).

		Brown needlefall in the same or next season									Green needlefall in the same or next season								
Climate variable		winter			summer			autumn			winter			summer			autumn		
Winter	rain%	.	.	.	.	.	.	.	.	.	.	.	.	.	.	.	.	.	.
	Δtemp	.	.	.	.	.	.	.	.	.	↑	↑	↑	↑	↑	↑	.	.	.
	Palmer	.	.	.	.	.	.	.	.	.	.	.	.	.	.	.	.	.	.
Summer	rain%	.	.	.	↓	↓	↓	↑	↑	.	.	.	.	.	.	↑	.	.	.
	Δtemp	↓	.	.	↓	↓	↓	.	.	.	.	.	.	.	.	.	.	↑	.
	Palmer	.	↑	↑	↓	↓	↓	↑	↑	.	.	.	.	.	.	.	.	.	.
Autumn	rain%	↓	↓	.	.	.	.	.	.	.	.	.	.	.	.	.	.	.	.
	Δtemp	.	.	.	↓	.	.	.	.	.	.	.	.	.	.	.	.	.	.
	Palmer	.	.	.	.	.	.	↑	↑	↑	.	.	.	.	.	.	.	.	.

Table 5. Hypothesis testing for the variables used in Eq. 2 for brown needlefall (Y_{ijk}) based on the Likelihood-ratio tests. N is the number of parameters, ΔN is the sequential increase in the number of parameters, –2LL is the –2ln(Likelihood), –2ΔLL is the sequential change in –2LL, and $p >$ –2ΔLL is the probability of –2ΔLL > $\chi^2_{n,0.05}$. For further details *see* the text above.

Step	Model	N	ΔN	–2LL	–2ΔLL	$p >$ –2ΔLL
1	$\ln(Y_{ijk}) = \beta_0$	1		2352		
2	$\ln(Y_{ijk}) = \beta_0 + e_{ijk}$	2	1	2291	61	< 0.0001
3	$\ln(Y_{ijk}) = \beta_0 + e_{ijk} + u_{ij}$	3	1	1952	339	< 0.0001
4	$\ln(Y_{ijk}) = \beta_0 + e_{ijk} + u_{ij} + \beta_{1i}$	11	8	1879	73	< 0.0001
5	$\ln(Y_{ijk}) = \beta_0 + e_{ijk} + u_{ij} + \beta_{1i} + \beta_{2i}p_j$	19	8	1857	22	0.00571

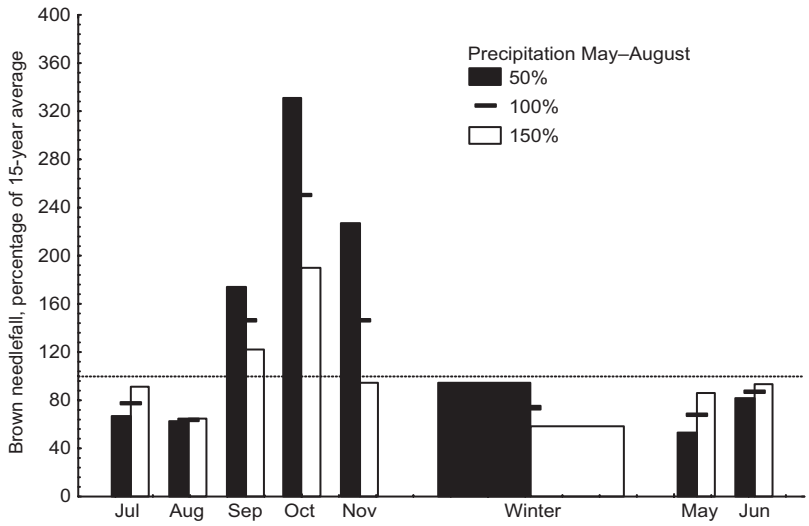

Fig. 2. Brown needlefall flux predicted with Eq. 2 for three alternative summer precipitation values: 50%, 100% and 150% of the 1961–1990 normal. The width of the bars represents the length of the sampling period. Correction factor for transformation bias = 1.26.

amount that comes a few months earlier than normal, but is an increase in the total brown needlefall. In Fig. 2, the 50% and 150% values of normal precipitation were selected to demonstrate the drought effect. These values were roughly the averages of the plot maxima and minima during the 15 years.

The results indicate that brown needlefall to some extent occurred as regional events. The random effect timepoint, u_{ij}, i.e. the correlation between plots sampled at the same point in time was affected by weighting by days. The variance estimate was 0.18, which gave an estimated correlation of 0.25 between samples taken in the same month from different plots. The correlation was 0.62 for the longer, winter samples. There appeared to be an antagonistic effect in the model between the drought effect on October needlefall and the random effect "timepoint", i.e. the disturbance effect common for all plots at every point of sampling. When this random effect was removed from the model, October became the month with the strongest relationship to summer drought. The explanation for this seems to be that in a number of years (1986, 1989, 1992 and 1997) brown needlefall had considerable peaks in October in all the plots, with mean values of 600, 550, 1210 and 440 kg ha^{-1} day^{-1}, respectively. The summers of these years were also dry, with periods of low precipitation or high temperatures. However, the synchronized October peaks at all plots can be confused with a random disturbance occurring in the entire region. By far the greatest peak in the data set, i.e. October 1992, was not well fit by the model. This peak appears to be caused by extremely dry June, with only 3%–20% of the normal precipitation, and temperatures 2–3 degrees above the normal. However, precipitation was close to normal for the entire summer, and our model did not pick up the effect of this drought because we used weather data for the entire summer.

One feature of the statistical model was the inclusion of temporal autocorrelation, i.e. that neighbouring sampling periods are more similar than those further apart. If such an autocorrelation is present, then in the hypothesis testing the observations cannot be treated as independent. By modelling this as a separate part of the model, it was no longer violating the hypothesis testing. An additional benefit is that it enabled a better understanding of the needlefall dynamic. The result was firstly that a significant autocorrelation in time was found, and secondly, it lasted for about one month. The covariance parameter ρ was estimated to be 0.96. This means that the autocorrelation between two observations that were one month (30 days), apart was 0.29. If they were 2 months (~61 days) apart the autocorrelation would be negligible, i.e. 0.08.

Two other random effects were initially included in the model, but were discarded. These

were the effects of 'plot' and the interaction 'plot × sampling period'. As expected, the first effect did not improve the model at all, because all data were initially recalculated to relative values for each plot, i.e. percentage values of the plot mean. The latter improved the model slightly. The improvement was significant, when using the likelihood ratio test (Schabenberger and Pierce 2002). However, it had almost no effect on hypothesis testing and parameter estimates for other effects in the model, and its variance estimate was of negligible order ($\sigma^2 = 0.02$), as compared with the other random effects in the model.

Green needlefall and weather conditions

Green needlefall constituted 16% of the total needlefall (Table 2). The correlation analyses indicated an association between high temperatures and increased green needlefall during winter and summer (Table 4). The strongest relationship was between mean temperature deviation and needlefall in the winter (Spearman's $r = 0.45$).

Equation 3 supported these findings, and all the variables used in the model were statistically significant at $p = 0.05$ (Table 6). Shedding of green needles mostly occurred in May (Fig. 3). Considerable increases in green needlefall were found in the winter and in May when the temperature in these periods were above normal. In November and in the winter, the model predicted close to zero needlefall in cool weather. November is of minor importance here because the absolute values were small. The estimated increase in May was considerable. Together, the results indicate that warm weather in the late autumn, winter and spring is likely to incite shedding of green needles. Because the winter period here is five months long, the aggregated amount of a slight increase in needle fall can be considerable.

The green needlefall had a tendency to occur as regional events, as found for brown needlefall. The random effect timepoint, u_{ij}, had a variance estimate of 0.20, which gave an estimated correlation of 0.11 between monthly samples (30 days) and 0.39 for winter samples (150 days). The autocorrelation in time lasted for about 2 months, i.e. slightly longer than for the brown needlefall. The covariance parameter ρ was estimated to be 0.976, which means that the autocorrelations between two observations one month (30 days) and three months apart were 0.48 and 0.11, respectively. As found for the brown needlefall, the two other random effects 'plot' and the interaction 'plot × sampling period' were discarded as their contributions to the model were non-significant.

Surplus needlefall and defoliation

Accumulated surplus of needlefall due to drought and warmth showed an overall increase during the years, in particular during 1989–1993 (Fig. 4). This was also the period with a marked increase in the defoliation in this part of Norway (Solberg 2004). During the first years, 1986–1989, the surplus of the needlefall was negative, because of moist summers and cold winters. This was also a period with only small changes in defoliation. The accumulated surplus of the needlefall for the entire period 1986–2001 was 77% of one year's average needlefall. Of this, the green and brown needlefall constituted 60% and 17%, respectively. The unusually mild

Table 6. Hypothesis testing for the variables used in Eq. 3 for green needlefall (Y_{ijk}) based on Likelihood-ratio tests. N is the number of parameters, ΔN is the sequential increase in the number of parameters, –2LL is –2ln(Likelihood), -2ΔLL is the sequential change in –2LL, and $p > -2\Delta$LL is the probability of $-2\Delta\text{LL} > \chi^2_{n,0.05}$. For further details *see* the text above.

Step	Model	N	ΔN	–2LL	-2ΔLL	$p > -2\Delta$LL
1	$\ln(Y_{ijk}) = \beta_0$	1		3069		
2	$\ln(Y_{ijk}) = \beta_0 + e_{ijk}$	2	1	2944	125	< 0.0001
3	$\ln(Y_{ijk}) = \beta_0 + e_{ijk} + u_{ij}$	3	1	2703	241	< 0.0001
4	$\ln(Y_{ijk}) = \beta_0 + e_{ijk} + u_{ij} + \beta_{1i}$	11	8	2623	80	< 0.0001
5	$\ln(Y_{ijk}) = \beta_0 + e_{ijk} + u_{ij} + \beta_{1i} + \beta_{2i} t_{ij}$	19	8	2604	19	0.01655

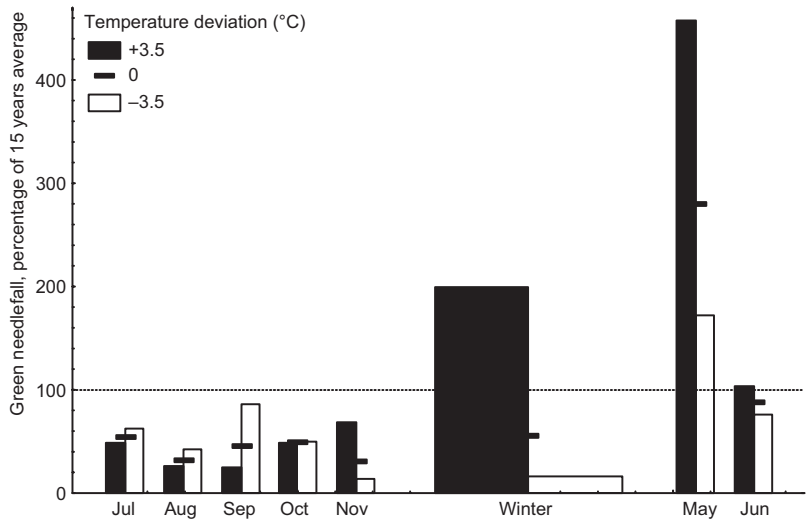

Fig. 3. Green needlefall flux predicted with Eq. 3 for three alternative temperature settings: –3.5, 0 and +3.5 °C deviation from the 1961–1990 normal. The widths of the bars represents the lengths of the sampling periods. Correction factor for transformation bias was 1.44.

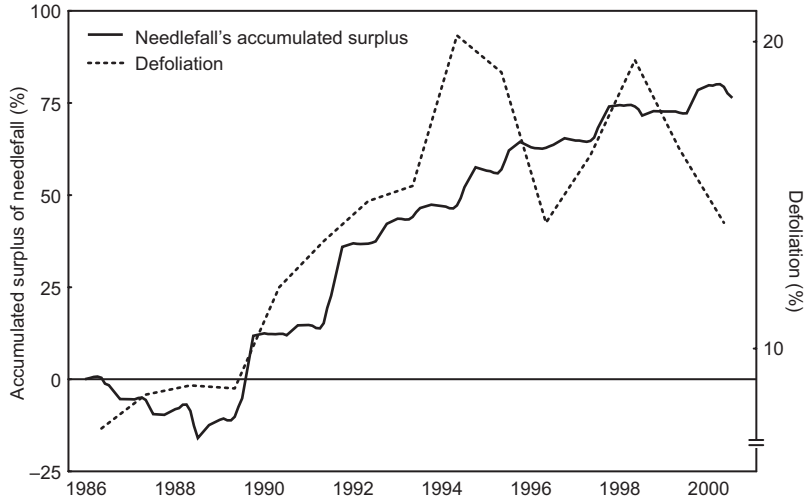

Fig. 4. Estimated accumulated surplus of needlefall due to unusually dry summers and unusually high temperatures, for the Level II plots in southeastern Norway during 1986–2000. The surplus is the difference between the needlefall modelled with the actual values of summer precipitation and temperature, minus the modelled needlefall that would have been the case had these weather variables been equal to the 1961–1990 normal values. The value 100 corresponds to one year's needlefall.

winters 1989, 1990 and 1992 alone contributed with 30 percentage units to the 77% surplus needlefall.

Discussion

General findings

Our results are in line with other studies. The mean needlefall flux was 3.6 kg ha^{-1} day^{-1}, with plot means ranging from 2.2 to 6.0 kg ha^{-1} day^{-1}. This corresponds to 80–219 g m^{-2}, which is similar to the range 33–331 g m^{-2} found in Finland (Saarsalmi *et al*. 2007). Our range corresponds to 803–2190 kg ha^{-1} year^{-1}, which is within the 530–6830 kg ha^{-1} year^{-1} range found for various conifer forest stands throughout Europe by Berg and Meentemeyer (2001). The annual cycle of needlefall, with a peak in late autumn and a peak

in spring was also found by Mork (1942), Gruber (1990), Heiniger and Schmid (1989) and Livsey and Barklund (1993).

Brown needlefall and weather conditions

The statistical analyses indicated an increase in brown needlefall after warm and dry summers. This was also found by Mork (1942), Gruber (1990) and Livsey and Barklund (1993). We observed the brown needlefall process after the dry summers of 1991 and 1992, and it was similar to the descriptions given by Heiniger and Schmid (1989) and Rehfuess and Rodenkirchen (1984). The needles of Norway spruce remained green until September followed by scattered yellow discoloration. Gradually, yellow turned brown, or red-brown, and heavy needlefall was observed mainly in October. This in general affected older needles, but also whole branches of higher order, in inner parts of the crown. Gruber (1990) explained the needlefall as a physiological response to water stress. When a needle dries up, the shrinkage of cells along the abscission layer causes the needle to tear off. However, we present here an alternative explanation for brown needlefall. Summer drought causes an increased needlefall; however, a delay of about 3 months between the drought and the increased needlefall in the autumn cannot be explained as a direct physiological tearing-off of the needles. The three-month delay might be a result of the slow work of weak pathogens, i.e. endophytic fungi causing accelerated needle senescence. The senescence is seen as a fast and gradual colour change from green via yellow to brown, followed by needle shedding. From our observations in the field this colour change typically varied from needle to needle and also varied within each needle, which could fit with the presence and work of endophytic fungi. In addition, entire branches and branchlets were dying completely, perhaps indicating the work of endophytic pathogens in the cambium. We observed a necrotic ring in the cambium around the base of such affected branches. A wide variety of endophytic fungi are found in spruce needles, such as *Phacidiopycnis* sp., *Sirococcus* sp., *Chalara* sp. and *Cistella acuum* (Koukol *et al*. 2012). Przybyl *et al*. (2008) found 54 species of fungi in freshly-fallen spruce needles. However, the most likely candidate for acting as the pathogen here is *Lophodermium piceae*. In a subset of the needlefall samples used in this study, Solheim (1989) found fruit bodies of *L. piceae* on around 40% of brown needles in the period October–winter. In Sweden, Livsey and Barklund (1993) obtained similar results. *Lophodermium piceae* frequently infects spruce needles, seen as an increasing number of infections during the first 3 years of the lifetime of a needle (Lehtijarvi and Barklund 2000). This shows that *L. piceae* can be present as a non-pathogenic fungus in the needles for a long time, while mycelial growth is postponed until needle senescence and death (Lehtijarvi and Barklund 2000), possibly acting weakly pathogenic after a period of drought or other types of stress. Other endophytic fungi may also act as weak pathogens, and perhaps there are regional differences. In Switzerland, Heiniger and Schmid (1989) found high frequencies of another endophytic fungus, *Tiarosporella parca*, on brown needles in the autumn. In a heavy brown needlefall event in Germany, *Rhizosphaera kalkhoffi* was suggested as a weak pathogen by Rehfuess and Rodenkirchen (1984).

Green needlefall and weather conditions

The statistical analyses indicated increased green needlefall in the winter and spring if the weather was mild or warm. The cause of this is uncertain. Most likely the needlefall was an instant response to warm weather, with increased transpiration from the needles while water supply was low. Alternatively, the high temperatures caused breaking of winter dormancy followed by frost damage. In both cases desiccation would be the result, and abscission as described by Gruber (1990) is likely to occur. Water loss in winter occurs both through stomata and through the cuticle (Grace 1990). Needlefall in winter and spring was linked to desiccation by high temperatures and wind by Diamandis (1979) and Klein (1985). Gruber (1990) found that green needles in winter were mainly torn off mechanically, while from April on they were shed after desiccation.

Surplus needlefall and defoliation

Our results suggest that in the studied region of Norway there was excess needlefall during the period 1986–2000 caused by unusually warm and dry weather. We expected to find an effect of dry summers on brown needlefall, because it was very evident and it has also been found by others. However, surprisingly, the surplus of green needlefall from warm winters has been of greater magnitude, and was likely to have played a more important role in the crown defoliation than the brown needlefall. The relationship between needlefall and defoliation was proven. It was clear that when needlefall increased considerably for some years from 1989, it corresponded to increased defoliation. The temporal development was similar in two other defoliation surveys in Norway, i.e. the national representative plots (Hylen and Larsson 2002) and the forest officers' plots (Solberg 2001), with increasing defoliation up to the year 1997 followed by a more stable period. In Denmark, Bille-Hansen and Hansen (2001) found relationships between defoliation and needlefall. Between-plot variation in the needlefall across Europe is also strongly explained by climatic variables (Berg and Meentemeyer 2001). For Norway spruce it explained 78% of the between-plot variation in the needlefall by actual evapotranspiration. Together this indicates that climate is a dominating factor in needlefall and likely also in defoliation.

A range of other factors are known to increase defoliation through increased needlefall, such as a fungal disease, abiotic damage like frost, or mechanical tearing-off of needles by storm. Defoliation caused by needlefall after direct SO_2 damage in combination with climatic factors was observed in the Ore Mountains in the Czech Republic (Lomsky and Sramek 2002). In this study, we only included drought or warmth as explanatory variables. However, because such effects often occur on a regional scale, the present models handle all such effects together as a random disturbance effect occurring for all plots at every point of time when sampling took place.

It is likely that the models underestimated the effect of drought and warmth on the needlefall. Firstly, the optimal variable for drought stress was not found. Clearly, the effect of the June 1992 drought on the brown needlefall in October was not caught by the model. The reason for this is that we used total summer precipitation in the model, and this was close to normal despite the June drought. Also, regressions will always underestimate a relationship when there is a random error in the explanatory variable (Webster 1997), which is likely to be the case for the precipitation variable. This also means that the estimated, seasonal variation with a normal peak in late autumn is affected partly by summer droughts, and the real seasonal variation in summers with normal precipitation is less pronounced than our results indicate.

Conclusion

In conclusion, the hypothesis that increased defoliation was caused by dry summers inciting heavy fall of brown needles in the following autumns was only partly supported. Dry summers were indeed followed by high peaks of brown needlefall. However, increased amounts of green needlefall during mild or warm winters and springs had apparently a stronger effect on the total needlefall and defoliation. The mean needlefall flux was 3.6 kg ha^{-1} day^{-1}, with considerable variation between plots due to site productivity and stand density. Brown needlefall had a regular seasonality with peaks in the autumn. The green needlefall peaked in May. Needlefall increased from warm and dry weather in general. Brown needlefall increased after warm and dry summers, while green needlefall increased from warm weather in the winter and spring. Increased needlefall from warmth and drought could well explain the increased defoliation observed during the 1980s and 1990s. Green needlefall was particularly high in mild winters. Altogether, a number of unusually dry summers and mild winters apparently caused enhanced needlefall and defoliation in Norway spruce in southeastern Norway during the study period 1986–2000.

Acknowledgements: We acknowledge the ministries of the agriculture and the environment, and the Norwegian research council for their financial support of the forest monitoring in Norway as well as this study.

References

Anon. 1989. *Manual on methodologies and criteria for harmonised sampling, assessment, monitoring and analysis of the effects of air pollution on forests'*. International Co-operative Programme on Assessment and Monitoring of Air Pollution Effects on Forests.

Anon. 1990. *SAS/STAT User's guide, version 6*, vol. 2, 4th ed. SAS Institute Inc., Cary, NC.

Aronsson A., Elowson S. & Forsberg N.G. 1978. Torkskador på gran i Västmanland. *Sveriges Skogvårdsförbunds Tidsskrift* 76: 441–456

Berg B. & Meentemeyer V. 2001. Litter fall in some European coniferous forests as dependent on climate: a synthesis. *Canadian Journal of Forest Research* 31: 292–301.

Bille-Hansen J. & Hansen K. 2001. Relation between defoliation and litterfall in some Danish *Picea abies* and *Fagus sylvatica* stands. *Scandinavian Journal of Forest Research* 16: 127–137.

Christiansen E. 1992. After-effects of drought did not predispose young *Picea abies* to infection by the bark beetle-transmitted blue-stain fungus *Ophiostoma polonicum*. *Scandinavian Journal of Forest Research* 7: 557–569.

Dambrine E., Carisey N., Pollier B. & Granier A. 1993. Effects of drought on the yellowing status and the dynamics of mineral elements in the xylem sap of declining spruce (*Picea abies* L.). *Plant and Soil* 150: 303–306.

DeVries W., Dobbertin M.H., Solberg S., Dobben H.F. & Schaub M. 2014. Impacts of acid deposition, ozone exposure and weather conditions on forest ecosystems in Europe: an overview. *Plant and Soil* 380: 1–45.

Diamandis S. 1979. "Top-dying" of Norway spruce, *Picea abies* (L.) Karst., with special reference to *Rhizosphaera kalkhoffi* Bubak. VI. Evidence related to the primary cause of "top-dying". *European Journal of Forest pathology* 9: 183–191.

ESRI 2001. *ArcGIS geographical information system*. Environmental Systems Research Institute, Redlands, USA.

Førland E. 1993. *Norwegian National Atlas: Annual precipitation (Map 3.1.1) and Monthly precipitation (Map 3.1.2)*. DNMI and Norwegian Mapping Authority.

Grace J. 1990. Cuticular water loss unlikely to explain treeline in Scotland. *Oecologia* 894: 64–68.

Gruber F. 1990. *Verzweigungssystem, Benadelung und Nadelfall der Fichte (Picea abies)*. Birkhäuser, Basel.

Heiniger U. & Schmid M. 1989. Association of *Tiarosporella parca* with needle reddening and needle cast in Norway spruce. *European Journal of Forest pathology* 19: 144–150.

Hentschel R., Rosner S., Kaylera Z.E., Andreassen K., Børja I., Solberg S., Tveito O.E., Priesack E. & Gessler A. 2014. Norway spruce physiological and anatomical predisposition to dieback. *Forest Ecology and Management* 322: 27–36.

Horntvedt R., Aamlid D., Rørå A. & Joranger E. 1992. Monitoring programme for forest damage. An overview of the Norwegian programme. *Norwegian Journal of Agricultural Sciences* 6: 1–17.

Hylen G. & Larsson J.Y. 2002. *National monitoring of forest vitality in Norway 1989–2001*. NIJOS rapport 1/2002.

Kandler O. & Innes J.L. 1995. Air pollution and forest decline in central Europe. *Environ Pollut* 90: 171–180.

Klein E. 1985. Nadelschütten im Winter. *Allgemeiner Forstzeitung* 40: 288–290.

Koukol O., Kolarik M., Kolarova Z. & Baldrian P. 2012. Diversity of foliar endophytes in wind-fallen *Picea abies* trees. *Fungal Diversity* 54: 69–77.

Lehtijarvi A. & Barklund P. 2000. Seasonal patterns of colonization of Norway spruce needles by *Lophodermium piceae*. *Forest Pathoogy* 30: 185–193.

Liebhold E. & Drechsler M. 1991. Schadenzustand und -entwicklung in den SO_2-geschädigten Fichtengebieten Sachsens. *Allgemeine Forstzeitung* 46: 492–494

Littell R.C., Milliken, G.A., Stroup, W.W. & Wolfinger R.D. 1996. *SAS System for mixed models*. SAS Institute Inc. Cary, NC.

Livsey S. & Barklund P. 1993. *Lophodermium picea* and *Rhizosphaera kalkhoffii* in fallen needles of Norway spruce (*Picea abies*). *European Journal of Forest pathology* 22: 204–216.

Lomsky B. & Sramek V. 2002. Damage of the fores stands in 1990's. In: Lomský B., Materna J. & Pfanz H. (eds.), *SO_2-pollution and forest decline in the Ore mountains*, Ministry of Agriculture of the Chech Republic, Forestry and Game Management Research Institute, Jiloviste-Strnady, pp. 139–155.

Lorenz M. 1995. International co-operative programme on assessment and monitoring of air pollution effects on forests — ICP forests. *Water Air and Soil Pollution* 85: 1221–1226.

Lorenz M., Augustin S., Becher G. & Förster M. 1997. *Forest condition in Europe. Results of the 1996 crown condition survey*. Technical Report, EC-UN/CEC, Brussels and Geneva.

Mork E. 1942. Om ströfallet i våre skoger. *Meddelelser fra det norske skogforsøksvesen* 29: 299–365.

Palmer W.C. 1965. *Meteorological drought*. U.S. Weather Bureau, Research Paper No. 45.

Przybyl K., Karolewski P., Oleksyn J., Labedzki A. & Reich P.B. 2008. Fungal diversity of Norway spruce litter: Effects of site conditions and premature leaf fall caused by bark beetle outbreak. *Microbial Ecology* 56: 332–340.

Rehfuess K.E. & Rodenkirchen H. 1984. Über die Nadelröte-Erkrankung der Fichte (*Picea abies* Karst.) in Süddeutschland. *Forstwissenschaftliche Centralblatt* 103: 248–262.

Roll-Hansen N. 2002. Ideological obstacles to scientific advice in politics? The case of "forest death" and "acid rain". *Makt- og demokratiutredningen*, rapport 48: 1–79

Rosner S., Svetlik J., Andreassen K., Børja I., Dalsgaard L., Evans R., Karlsson B & Solberg S. 2014. Wood density as a predictive trait for vulnerability to cavitation in Norway spruce trunks: lessons from healthy and declining trees after the 2003 and 2006 heat waves. *Canadian Journal of Forest Research* 44: 154–161.

Saarsalmi A., Starr M., Hokkanen T., Ukonmaanaho L., Kukkola M., Nöjd P. & Sievänen R. 2007. Predicting annual canopy litterfall production for Norway spruce (*Picea*

abies (L.) Karst.) stands. *Forest Ecology and Management* 242: 578–586.

Schabenberger O. & Pierce F.J. 2002. *Contemporary statistical models for the plant and soil sciences*. CRC Press, Boca Raton.

Solberg S. & Tørseth K. 1997. Crown condition of Norway spruce in relation to sulphur and nitrogen deposition and soil properties in Southeast Norway. *Environmental Pollution* 96: 19–27.

Solberg S. 2001. Forest officers' monitoring plots. Vitality survey 2001. *Rapport fra Skogforsk* 9/01: 1–20.

Solberg S. 2004. Summer drought — a driver for crown condition and mortality of Norway spruce in Norway. *Forest Pathology* 34: 93–104

Solheim H. 1989. Fungi on spruce needles in Norway. II. Notes about *Tiarosporella parca*. *European Journal of Forest pathology* 19: 189–191.

Spiecker H. 1986: Das Wachstum der Tannen und Fichten auf Plenterwald-Versuchsflächen des Schwarzwaldes in der Zeit von 1950 bis 1984. *Allgemeine Forst und Jagd Zeitung* 157: 152–164.

Tveito O.E., Førland E.J., Heino R., Hanssen-Bauer I., Alexandersson H., Dahlström B., Drebs A., Kern-Hansen C., Jónsson T., Vaarby-Laursen E. & Westman Y. 2000. *Nordic temperature maps*. DNMI Report 09/00, KLIMA.

Webster R. 1997. Regression and functional relations. *European Journal of Soil Science* 48: 557–566.

Wehrmann J. 1961. Die Auswirkung der Trockenheit von 1959 auf die Närhelementversorgung bayerischer Kiefernbestände. *Forswissenschaftliche Centralblatt* 80: 272–287.

Wentzel V.K.F. 1982. Ursachen des Waldsterbens in Mitteleuropa. *Allgemeine Forstzeitung* 37: 1365–1368

Whitney R.D., Timmer V.R. 1983. *Chlorosis in planted white spruce at Limestone Lake*. Inf. Rep. D-X-346, Ontario Department of Environment, Canadian Forest Service, Sault Ste. Marie, Ontario.

Worrell R. 1983. Damage by the spruce bark beetle in South Norway 1970–80: A survey, and factors affecting its occurrence. *Meddelelser fra det norske skogforsøksvesen* 38: 1–34.